

Measurement of the $\gamma\gamma$ Partial Width of the χ_2 Charmonium Resonance

T. A. Armstrong,⁽⁶⁾ D. Bettoni,⁽²⁾ V. Bharadwaj,⁽¹⁾ C. Biino,⁽⁷⁾ G. Borreani,⁽²⁾ D. Broemmelsiek,⁽⁴⁾ A. Buzzo,⁽³⁾ R. Calabrese,⁽²⁾ A. Ceccucci,⁽⁷⁾ R. Cester,⁽⁷⁾ M. Church,⁽¹⁾ P. Dalpiaz,⁽²⁾ P. F. Dalpiaz,⁽²⁾ R. Dibenedetto,⁽⁷⁾ D. Dimitroyannis,⁽⁵⁾ M. Fabbri,⁽²⁾ J. Fast,⁽⁴⁾ A. Gianoli,⁽²⁾ C. M. Ginsburg,⁽⁵⁾ K. Gollwitzer,⁽⁴⁾ A. Hahn,⁽¹⁾ M. A. Hasan,⁽⁶⁾ S. Hsueh,⁽¹⁾ R. Lewis,⁽⁶⁾ E. Luppi,⁽²⁾ M. Macrí,⁽³⁾ A. M. Majewska,⁽⁶⁾ M. Mandelkern,⁽⁴⁾ F. Marchetto,⁽⁷⁾ M. Marinelli,⁽³⁾ J. Marques,⁽⁴⁾ W. Marsh,⁽¹⁾ M. Martini,⁽²⁾ M. Masuzawa,⁽⁵⁾ E. Menichetti,⁽⁷⁾ A. Migliori,⁽⁷⁾ R. Mussa,⁽⁷⁾ S. Palestini,⁽⁷⁾ M. Pallavicini,⁽³⁾ N. Pastrone,⁽⁷⁾ C. Patrignani,⁽³⁾ J. Peoples, Jr.,⁽¹⁾ L. Pesando,⁽⁷⁾ F. Petrucci,⁽²⁾ M. G. Pia,⁽³⁾ S. Pordes,⁽¹⁾ P. A. Rapidis,⁽¹⁾ R. Ray,^{(1),(5)} J. Reid,⁽⁶⁾ G. Rinaudo,⁽⁷⁾ B. Rocuzzo,⁽⁷⁾ J. Rosen,⁽⁵⁾ A. Santroni,⁽³⁾ M. Sarmiento,⁽⁵⁾ M. Savrié,⁽²⁾ A. Scalisi,⁽³⁾ J. Schultz,⁽⁴⁾ K. K. Seth,⁽⁵⁾ A. Smith,⁽⁴⁾ G. A. Smith,⁽⁶⁾ M. Sozzi,⁽⁷⁾ S. Trokenheim,⁽⁵⁾ M. F. Weber,⁽⁴⁾ S. Werkema,⁽¹⁾ Y. Zhang,⁽⁶⁾ J. Zhao,⁽⁵⁾ and G. Zioulas⁽⁴⁾

(E760 Collaboration)

⁽¹⁾Fermi National Accelerator Laboratory, Batavia, Illinois 60510⁽²⁾Istituto Nazionale di Fisica Nucleare and University of Ferrara, 44100 Ferrara, Italy⁽³⁾Istituto Nazionale di Fisica Nucleare and University of Genoa, 16146 Genoa, Italy⁽⁴⁾University of California at Irvine, Irvine, California 92717⁽⁵⁾Northwestern University, Evanston, Illinois 60208⁽⁶⁾Pennsylvania State University, University Park, Pennsylvania 16802⁽⁷⁾Istituto Nazionale di Fisica Nucleare and University of Turin, 10125 Turin, Italy

(Received 2 October 1992)

The E760 Collaboration has studied the reaction $\bar{p}p \rightarrow \chi_2 \rightarrow \gamma\gamma$ using a hydrogen gas jet target in the Fermilab antiproton accumulator ring. The following values are obtained for the branching ratio and partial width to two photons; $B(\chi_2 \rightarrow \gamma\gamma) = (1.60 \pm 0.45) \times 10^{-4}$ and $\Gamma(\chi_2 \rightarrow \gamma\gamma) = 321 \pm 95$ eV.

PACS numbers: 14.40.Gx, 13.40.Hq, 13.75.Cs

This paper reports a measurement of the $\gamma\gamma$ decay of the $\chi_2(^3P_2)$ charmonium resonance formed in $\bar{p}p$ annihilation. Within the framework of perturbative QCD [1], the ratio of the partial widths $\Gamma(\chi_2 \rightarrow gg)/\Gamma(\chi_2 \rightarrow \gamma\gamma)$ can be related to the coupling constant α_s at the charm quark mass.

Experiment E760 utilizes an internal hydrogen gas jet target which intersects a cooled ($\delta P/P \leq 2 \times 10^{-4}$) beam of antiprotons circulating in the accumulator ring at Fermilab. The interaction region is determined transversely by the beam and longitudinally by the gas jet, both of which are round with diameters of 5 mm and 6.3 mm (95% containment), respectively. The detector [2] is optimized for the identification of the $e^+e^- + X$ and multi- γ final states. It covers the complete azimuth (ϕ) and the polar angle (θ) from 2° to 70° . It consists of three sets of scintillator hodoscopes, two in the central region (H1, H2) and the third covering the forward region (FCV), a multicell threshold gas Čerenkov counter for electron identification, several layers of tracking detectors, and central (CCAL) and forward (FCAL) electromagnetic calorimeters.

For the identification of the $\gamma\gamma$ final state the central calorimeter [3] is the essential part of the detector. It must distinguish between $\gamma\gamma$ events and the large background from hadronic processes—in particular

$\bar{p}p \rightarrow \pi^0\pi^0$, $\bar{p}p \rightarrow \pi^0\gamma$, and $\bar{p}p \rightarrow \pi^0\eta$ —which have cross sections up to 10^3 times that of the $\gamma\gamma$ channel. The 1280 module lead glass shower counter array, 20 counters in θ by 64 counters in ϕ , is arranged in a pointing geometry and covers the region $11^\circ \leq \theta \leq 70^\circ$. The average rms angular resolution is 7 mrad in θ and 11 mrad in ϕ . The average rms energy resolution is $6.0\%/\sqrt{E(\text{GeV})} + 1.4\%$.

The E760 Collaboration has collected a total integrated luminosity of 2.58 pb^{-1} at the χ_2 formation energy, $\sqrt{s} \approx 3556 \text{ MeV}$. The $\gamma\gamma$ background is measured using 23.3 pb^{-1} of data taken at various values of \sqrt{s} from 3523 MeV to 3686 MeV. These data were collected during energy scans for other charmonium states, in particular the $h_c(^1P_1)$, η'_c , and ψ' .

The luminosity is obtained by counting recoil protons from forward elastic scattering with a silicon detector located at $\theta = 86.5^\circ$. The luminosity is extracted from knowledge of the $\bar{p}p$ elastic cross section and the detector acceptance. The estimated error in the absolute luminosity, $\pm 5.3\%$, is included as a systematic error in this measurement.

The trigger for events with all neutral final states is based on fast analog sums from the central calorimeter. It requires that two octants of the central calorimeter, separated by $\geq 90^\circ$ in azimuth, have recorded energies above $\sim 60\%$ of the values expected for a two-body de-

cay (the PBG1 requirement) [4]. Events with charged particles are rejected by requiring no hits in the H1 or FCV scintillator counters. There are two sources of inefficiency in this trigger. The first comes from the PBG1 requirement and the other from the random veto of neutral events due to the high rate of charged particles in the scintillator counters. The PBG1 efficiency is found to be $> 98\%$ from analysis of $\bar{p}p \rightarrow J/\psi \rightarrow e^+e^-$ events collected with a trigger which uses only the hodoscope and Čerenkov data. The inefficiency due to the charged particle veto is measured by removing the veto requirement from the trigger, reconstructing $\bar{p}p \rightarrow \pi^0\pi^0$ events, and determining how often the trigger bits for the vetoes are set, with a correction for Dalitz decays and conversions in the beam pipe. The data used to measure this inefficiency were collected with an instantaneous luminosity of $3.5 \times 10^{30} \text{ cm}^{-2} \text{ s}^{-1}$ while the data used in the $\chi_2 \rightarrow \gamma\gamma$ analysis were collected at luminosities in the range $(2.5\text{--}6.2) \times 10^{30} \text{ cm}^{-2} \text{ s}^{-1}$. The cross section for $\gamma\gamma$ candidates (after preliminary cuts) binned by instantaneous luminosity shows no luminosity dependence at the 3% level. The trigger efficiency is determined to be $\epsilon_{\text{trigger}} = 0.89 \pm 0.03 \pm 0.03$. For events passing the hardware trigger, the calorimeter data are read into online processors where a simplified clustering algorithm is applied and the invariant masses of all cluster pairs ($M_{\gamma\gamma}$) are calculated. Events with any $M_{\gamma\gamma} \geq 2.0 \text{ GeV}/c^2$ are recorded on tape.

The central calorimeter clustering algorithm [5] forms 3 block by 3 block clusters around all local maxima in the detector, i.e., blocks with more energy than their eight nearest neighbors. Energy thresholds of 5 MeV for the central blocks and 20 MeV for the 9 block regions are used. An energy weighted average position is found for the cluster and a correction is applied based on a parametrization of the transverse electromagnetic shower profile. Each coordinate (θ, ϕ) is treated independently, with the parameters determined empirically using electrons from J/ψ decay and test beam data. When two clusters overlap, the energy of the blocks in the overlap region is shared between them using an iterative procedure. The transverse shower profile parametrization is used in determining the fraction of energy assigned to each cluster. The procedure is iterated until the cluster centroids and cluster energies are stable at the level of the detector resolution.

The symmetric decay of an energetic π^0 can produce a hit pattern with only one local maximum, and hence forms only a single cluster. To identify such cases a *mass* is calculated for each cluster,

$$m = \sqrt{\left(\sum_i E_i\right)^2 - \left(\sum_i \mathbf{p}_i\right)^2}, \quad (1)$$

where E_i is the energy deposited in the i th block, $\mathbf{p}_i = E_i \hat{\mathbf{x}}_i$, and $\hat{\mathbf{x}}_i$ is the unit vector from the interaction point to the center of the i th block. Clusters from symmet-

ric π^0 decays give values near the mass of the π^0 , while clusters from single photons have smaller *mass* values. Figure 1 shows the *mass* distributions for clusters from J/ψ electrons and for clusters from $\bar{p}p \rightarrow \pi^0\pi^0$ events. The low *mass* clusters from π^0 's in Fig. 1 are due to photons which are well separated in the calorimeter. Any cluster with $m \geq 100 \text{ MeV}/c^2$ is split into two clusters, each representing an individual photon from the π^0 . It is kinematically impossible for the two photons from a π^0 to strike blocks sharing a side, so the corner block of the original 3 by 3 cluster with the highest energy is used as the central block for the second cluster. The iterative energy sharing procedure described above is used to determine the cluster energies and positions. A 5 by 5 grid is used for these clusters to improve position resolution.

Spurious clusters, produced primarily by the tails of signals from earlier interactions, are identified using 160 summed signals (20 in θ by 8 in ϕ), provided by the neutral trigger system [4], latched with a 30 ns gate. This system provides accurate classification of clusters above 200 MeV as in time or out of time, while below this energy they remain undetermined.

Candidate events are selected that have two central calorimeter clusters (in time) with an invariant mass $M_{\gamma\gamma} \geq 2.5 \text{ GeV}/c^2$. Up to two additional clusters, classified as out of time or undetermined, are allowed in the central calorimeter. No clusters are allowed in the forward calorimeter. A four constraint kinematical fit to the $\gamma\gamma$ hypothesis is done and events with a fit probability $\text{C.L.} \leq 5 \times 10^{-3}$ are rejected. An invariant mass cut at $\pm 10\% \sqrt{s}$ about the center of mass energy is imposed, corresponding to 3σ of the mass resolution obtained for $J/\psi \rightarrow e^+e^-$ and $\psi' \rightarrow e^+e^-$ events using only the calorimeter information. The masses calculated by pairing any additional clusters with each of the high energy clusters associated with the $\gamma\gamma$ candidate are plotted in Fig. 2. Events with any mass in the π^0 (80–170 MeV/c^2) or η (410–690 MeV/c^2) window are rejected. These windows correspond to $\approx \pm 2\sigma$ of the mass resolution. The inset in Fig. 2 shows the η mass region after

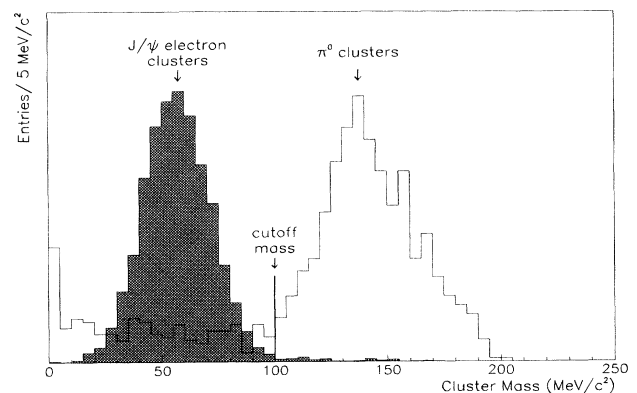


FIG. 1. Cluster *mass* of showers in the calorimeter.

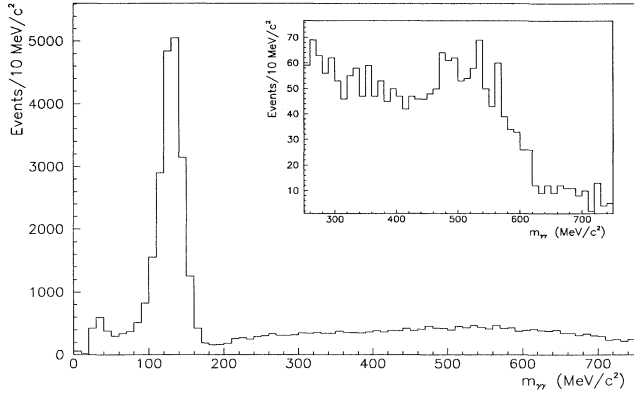


FIG. 2. Invariant mass of extra clusters with $\gamma\gamma$ candidate clusters.

the removal of events with a π^0 , indicating that there is a small contribution of events with an η .

Figure 3 shows the center of mass angular distributions for the remaining $\gamma\gamma$ candidates at the χ_2 and for the background data taken at $\sqrt{s} \approx 3525$ MeV (scaled to the luminosity taken at the χ_2 and corrected for the energy dependence of the background). The expected angular distribution for $\bar{p}p \rightarrow \chi_2 \rightarrow \gamma\gamma$ events, discussed below, is shown in the inset. Because of the rapid increase of the background with $|\cos\theta^*|$, the acceptance is restricted to the region $|\cos\theta^*| \leq 0.40$. Various values of this cut from $|\cos\theta^*| \leq 0.25$ to $|\cos\theta^*| \leq 0.50$ give consistent results. The results of this analysis are reported in Table I and displayed in Fig. 4. The data taken at $\sqrt{s} \approx 3525$ MeV have been combined in Table I and Fig. 4.

Monte Carlo simulations were used to estimate feed-down to the 2γ background from the direct 3γ decays of the ψ' and $h_c(1P_1)$, and from the radiative decays $\psi' \rightarrow \eta_c'\gamma$, $\psi' \rightarrow \chi_2\gamma$, $\psi' \rightarrow \chi_0\gamma$, $\psi' \rightarrow \eta_c\gamma$, and $h_c(1P_1) \rightarrow \eta_c\gamma$, with the daughter decaying to two photons. We expect contributions of < 1 event (of 14) in the data taken at the ψ' , $\sqrt{s} = 3686$ MeV and ≈ 1 event (of 204) in the

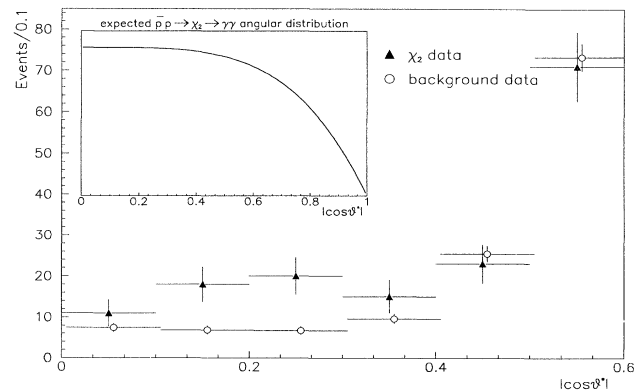


FIG. 3. Center of mass angular distribution of $\gamma\gamma$ candidates.

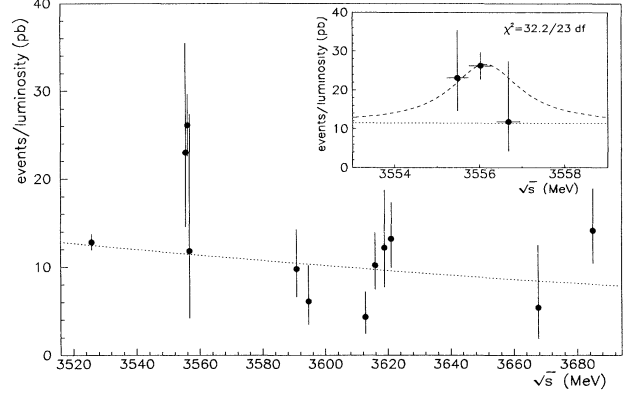


FIG. 4. Measured $\gamma\gamma$ cross section for the final data set (not corrected for efficiency and acceptance).

data taken at the $h_c(1P_1)$, $\sqrt{s} \approx 3525$ MeV.

The analysis efficiency has been measured using background free samples of $\psi' \rightarrow e^+e^-$ and $J/\psi \rightarrow e^+e^-$ events, selected using the hodoscopes and the Čerenkov data. These events are indistinguishable from $\gamma\gamma$ events in the calorimeter. The efficiencies calculated from the ψ' and two J/ψ samples are in good agreement. The efficiency of the analysis of these data, prior to the acceptance cut, is $\epsilon_{\text{analysis}} = 0.79 \pm 0.02 \pm 0.04$.

The angular distribution for the reaction $\bar{p}p \rightarrow \chi_2 \rightarrow \gamma\gamma$ is needed in order to extract the partial width $\Gamma(\chi_2 \rightarrow \gamma\gamma)$ from a measurement over the restricted angular region $|\cos\theta^*| \leq 0.40$. Because of the limited statistics of the data and the strong angular dependence of the background we are unable to extract the angular distribution directly. From the analysis of the reaction $\bar{p}p \rightarrow \chi_2 \rightarrow J/\psi \gamma \rightarrow e^+e^- \gamma$ [6] we find that the initial state is dominated by helicity=1, with an upper limit (90% C.L.) of 22% for the helicity=0 component. Nonrelativistic models predict that the decay $\chi_2 \rightarrow \gamma\gamma$ is purely helicity=2. With relativistic corrections the helicity=0 component is predicted to be $\leq 5\%$ of the partial width [7, 8]. If we

TABLE I. Final $\gamma\gamma$ candidates.

\sqrt{s} (MeV)	Events	$\int \mathcal{L}$ (pb $^{-1}$)	Events/ $\int \mathcal{L}$ (pb)
3522.7–3527.0	204	15.893	12.8
3555.3	7	0.304	23.0
3555.9	55	2.103	26.2
3556.6	2	0.169	11.8
3590.8	9	0.924	9.7
3594.6	5	0.827	6.0
3612.8	5	1.167	4.3
3615.9	13	1.276	10.2
3618.9	7	0.575	12.2
3621.1	16	1.216	13.2
3667.7	2	0.372	5.4
3686.0	14	0.995	14.1

TABLE II. Comparison with other measurements and theory.

	$\Gamma(\chi_2 \rightarrow \gamma\gamma)$ (keV)	$B(\chi_2 \rightarrow \gamma\gamma)$ (10^{-4})
Experiment		
E760	$0.32 \pm 0.08 \pm 0.05$	$1.6 \pm 0.4 \pm 0.2$
R-704 [11]	$2.9^{+1.3}_{-1.0} \pm 1.7^a$	$11^{+5}_{-4} \pm 4^a$
CLEO [12]	< 1.0 (95% C.L.)	
VENUS [13]	< 4.2 (95% C.L.)	
TPC [14]	< 4.2 (95% C.L.)	
Crystal Ball [15]	2.8 ± 2.0	
DASP [10]	< 1.6 (90% C.L.)	
Theory		
PQCD [1]	0.81 ± 0.15^b	
BA [8]	0.56	
BBL [16]		4.1 ± 1.1 ($\pm 36\%$)

^aThis result uses an isotropic angular distribution and $\Gamma(\chi_2) = 2.6^{+1.4}_{-1.0}$ MeV.

^bUsing $\Gamma(\chi_2 \rightarrow gg) = 1.71 \pm 0.21$ MeV and $\alpha_s = 0.276 \pm 0.014$.

assume pure helicity=1 in the initial state and pure helicity=2 in the final state, then the angular distribution assumes the simple form $W(\theta^*) = \frac{5}{4}[1 - \cos^4 \theta^*]$. Integrating over $|\cos \theta^*| \leq 0.4$, the fraction of the total cross section observed is 0.50 ± 0.02 , where the estimated error is associated with the uncertainties in the neglected helicity=0 components.

A maximum likelihood analysis of the data was performed using a power law dependence for the background, $\sigma_{\text{bkg}} = A(\sqrt{s})^B$ and two Breit-Wigner line shapes, one for the χ_2 resonance and one for a (hypothetical) η'_c resonance [9], convolved with the beam energy distribution. The mass and total width of the χ_2 resonance were fixed at $M = 3556.15$ MeV and $\Gamma = 1.98$ MeV, the values obtained from our analysis of the radiative decay $\chi_2 \rightarrow J/\psi \gamma$ [2]. The η'_c width was fixed at 5 MeV, while its mass and branching ratio product were free parameters. The data and fitted curve in the χ_2 region are shown in the inset in Fig. 4.

Several checks were made to estimate the systematic error due to background subtraction. The mass and total width of the χ_2 were varied within their respective errors. The total width of the η'_c was varied within reasonable limits (2 MeV to 15 MeV), and the η'_c resonance was removed from the fit. As a conservative treatment of the ≤ 1 feed-down events predicted at the ψ' and in the 1P_1 region, 3 events were removed at each of these points. We find that

$$B(\chi_2 \rightarrow \bar{p}p)B(\chi_2 \rightarrow \gamma\gamma) = (1.60 \pm 0.39 \pm 0.16) \times 10^{-8}. \quad (2)$$

Using $B(\chi_2 \rightarrow \bar{p}p) = (1.00 \pm 0.10) \times 10^{-4}$ and $\Gamma(\chi_2) = 2.00 \pm 0.18$ MeV [10] we obtain

$$B(\chi_2 \rightarrow \gamma\gamma) = (1.60 \pm 0.39 \pm 0.23) \times 10^{-4}, \quad (3)$$

$$\Gamma(\chi_2 \rightarrow \gamma\gamma) = 321 \pm 78 \pm 54 \text{ eV}. \quad (4)$$

A comparison of our results with previous measurements and with theoretical predictions appears in Table II.

Perturbative QCD expressions for the decay rates of charmonium into gluons and photons with next-to-lowest-order corrections can be found in Ref. [1]. The strong coupling constant $\alpha_s(m_c)$ can be derived from the ratio

$$\frac{\Gamma(\chi_2 \rightarrow gg)}{\Gamma(\chi_2 \rightarrow \gamma\gamma)} = \frac{9\alpha_s^2}{8\alpha^2} \left[\frac{1 - 2.2\alpha_s/\pi}{1 - 16\alpha_s/3\pi} \right]. \quad (5)$$

Using this measurement of the $\gamma\gamma$ width and our value of $\Gamma(\chi_2 \rightarrow gg) = 1.71 \pm 0.21$ MeV [2], a value $\alpha_s(m_c) = 0.36 \pm 0.04$ is obtained from the expression above. It should be noted that the lowest-order correction to the two photon rate of the χ_2 is very large, $[1 - 16\alpha_s/3\pi] = 0.4$ for $\alpha_s = 0.36$, and that potentially large relativistic corrections have not been taken into account.

We gratefully acknowledge the technical support from our collaborating institutions and the outstanding contribution of the Fermilab Accelerator Division. This work was funded by the U.S. Department of Energy, the National Science Foundation, and the Italian Istituto di Fisica Nucleare.

- [1] W. Kwong *et al.*, Phys. Rev. D **37**, 3210 (1988), and references therein.
- [2] T. A. Armstrong *et al.*, Nucl. Phys. **B373**, 35 (1992).
- [3] L. Bartoszek *et al.*, Nucl. Instrum. Methods Phys. Res., Sect. A **301**, 47 (1991).
- [4] R. Ray *et al.*, Nucl. Instrum. Methods Phys. Res., Sect. A **307**, 254 (1991).
- [5] J. Fast, Ph.D. thesis, University of California, Irvine, 1992.
- [6] T. A. Armstrong *et al.* (to be published).
- [7] Z. P. Li *et al.*, Phys. Rev. D **43**, 2161 (1991).
- [8] T. Barnes and E. Ackleh, Report No. ORNL-CCIP-92-05, UTK-92-3 (to be published).
- [9] The data taken in the interval $\sqrt{s} = 3612\text{--}3621$ MeV were part of a search for the η'_c resonance. The resonance was not observed, but a contribution from its $\gamma\gamma$ decay cannot be excluded and therefore we include it in this analysis.
- [10] Particle Data Group, Review of Particle Properties, Phys. Rev. D **45**, S1 (1992).
- [11] C. Baglin *et al.*, Phys. Lett. B **187**, 191 (1987).
- [12] W. Chen *et al.*, Phys. Lett. B **243**, 169 (1990).
- [13] S. Uehara *et al.*, Phys. Lett. B **266**, 188 (1991).
- [14] H. Aihara *et al.*, Phys. Rev. Lett. **60**, 2355 (1988).
- [15] R. Lee, Ph.D. thesis, SLAC, 1985, p. 282.
- [16] G. Bodwin *et al.*, Phys. Rev. D **46**, 1914 (1992).